Nuclear effects on ion heating within the small-angle charged-particle elastic-scattering regime

A. Andrade and G. M. Hale
Los Alamos National Laboratory, Mail Stop B243, Los Alamos, New Mexico 87545
(Received 18 July 1983)

The effects of nuclear forces (in contrast to pure Coulomb interaction) on the ion heating rate which results from small-angle scattering processes between charged particles in plasmas are investigated within the framework of Fokker-Planck theory. These effects are included through the addition of analytic Coulomb-nuclear interference and nuclear elastic cross sections in the scattering integrals of the dynamical friction coefficient and dispersion tensor. It is found that corrections to traditional Fokker-Planck predictions of the ion-ion energy exchange rate can be calculated and that these corrections are sensitive to the choice of the maximum scattering angle defining the cutoff between small- and large-angle scattering.

I. INTRODUCTION

The Fokker-Planck equation[1] has traditionally been used to calculate the energy exchange between charged particles which takes place in small-angle elastic scattering in plasmas, taking into account only the long-range Coulomb (Rutherford) interaction. Here the effects of nuclear forces on the small-angle ion-ion energy exchange, as manifested through analytic Coulomb-nuclear and nuclear elastic-scattering cross sections, will be investigated by means of a generalized Fokker-Planck equation.

The motivation for this work is apparent from considering the behavior of the ratio σ/σ_R for some typical interacting charged particle pairs as a function of the center-of-mass (c.m.) scattering angle. Here σ is the total differential elastic-scattering cross section and is defined to be the sum $\sigma_R+\sigma_{\rm NI}$, i.e., the sum of the Rutherford component and a combination $\sigma_{\rm NI}$ of the Coulomb-nuclear interference and nuclear elastic components. Figures 1—4 show R-matrix calculations[2] for σ/σ_R that give good representations of cross-section measurements[3–9] for deuterons elastically scattered from ^{2}H, ^{3}H, and ^{4}He, and for tritons elastically scattered from ^{4}He. For energies of a few MeV, the calculations show significant deviations from Rutherford scattering at angles below the smallest angle that has been measured, which is approximately 30°. In the case of D-T scattering, for example (Fig. 2), it is seen that the scattering cross section becomes an order of magnitude greater than σ_R in the small-angle scattering regime ($\theta \lesssim 30°$) for incident energies near 5 MeV. Hence, since it is not uncommon to have ions created quasicon-

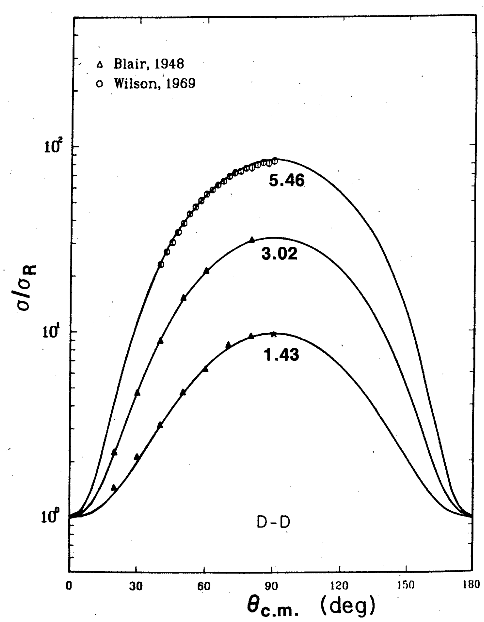

FIG. 1. The ratio of differential total to Rutherford elastic-scattering cross sections for ^{2}H on ^{2}H as a function of the center-of-mass scattering angle.

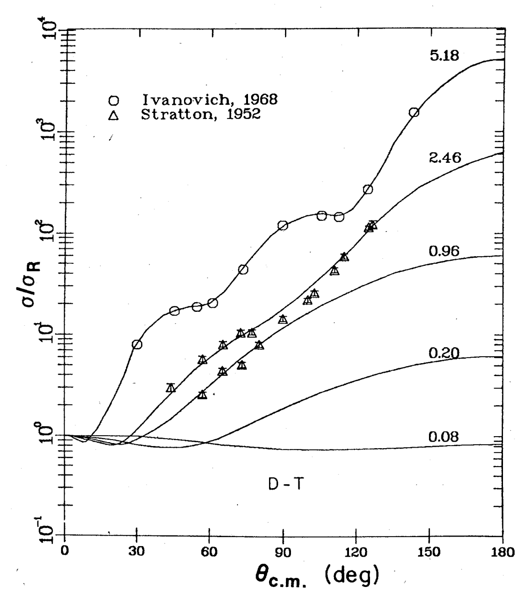

FIG. 2. The ratio of differential total to Rutherford elastic-scattering cross sections for ^{2}H on ^{3}H as a function of the center-of-mass scattering angle.

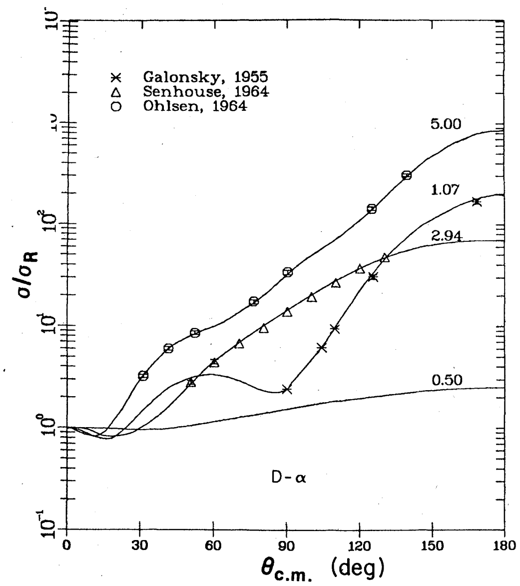

FIG. 3. The ratio of differential total to Rutherford elastic-scattering cross sections for ^2H on ^4He as a function of the center-of-mass scattering angle.

tinuously into this energy range in a reacting plasma, it is of interest to estimate the effects of these nuclear processes on the ion-ion heating rates that result within the small-angle scattering regime.

In the analysis to follow, it will be shown that the ion-ion energy exchange rate predicted by the generalized Fokker-Planck theory is sensitive to the cutoff angle θ_{max} which defines the onset of large-angle scattering. Previously, in Fokker-Planck theory that accounted for Coulomb interaction only, it was found that the results of ion slowing calculations were relatively insensitive to the choice of this cutoff.[10] This results from the fact that the scattering integrals in the dynamical friction coefficient and dispersion tensor can be evaluated in terms of a single parameter known as the Coulomb logarithm which, in turn, depends only weakly on the logarithm of $\sin(\theta_{max}/2)$. In the generalized theory, the evaluation of the scattering integrals will also yield the same logarithmic terms for the Rutherford part of the cross sections but, in addition, it will yield terms attributable to σ_{NI} which are more sensitive to θ_{max}.

The inequality $\theta_{max} \lesssim 30°$ mentioned above in specifying a range of small-angle scattering neither represents a canonical range of angles which differentiates between small- and large-angle scattering nor defines a range over which the Fokker-Planck equation is known to be strictly valid. Rather, it is a range over which the authors believe that a reasonable variation in nuclear effects can be demonstrated. The matter of specifying a θ_{max} more precisely and, thereby, of defining the angular range of validity of the Fokker-Planck equation, remains to be researched. It is interesting to note, however, that since experimental values of the elastic-scattering cross sections for many charged particle pairs do not exist for values $\theta \lesssim 30°$, and that since it is not strictly valid to assume that σ is pure Rutherford in this range, this formulation provides for a smooth transition between small- and large-angle ion slowing calculations. Large-angle ion slowing calculations requiring Monte Carlo techniques, for example, could begin at precisely the cutoff angle which is ultimately chosen for this theory.

Although the most important consequences of elastic nuclear collisions are manifested in the direct ion heating that occurs with the production of secondary generations of energetic ions through large-angle scattering, the intent of this work is to develop and investigate a complete calculational formalism in small-angle ion slowing theory through the inclusion of the entire elastic-scattering cross section in Fokker-Planck theory. Large-angle scattering in plasmas has been researched extensively elsewhere[11–13] and will not be addressed further in this paper.

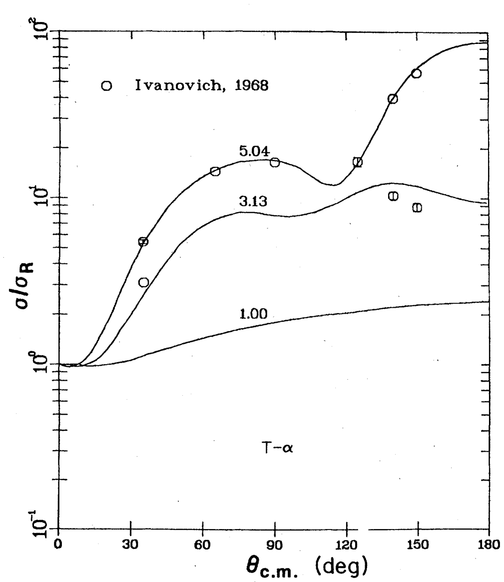

FIG. 4. The ratio of differential total to Rutherford elastic-scattering cross sections for ^3H on ^4He as a function of the center-of-mass scattering angle.

II. A GENERALIZED FOKKER-PLANCK EQUATION

The effects of Coulomb-nuclear interference and nuclear elastic small-angle scattering on ion-ion energy exchange can be investigated through the Fokker-Planck equation by generalizing the scattering integrals in the dynamical friction coefficient and the dispersion tensor to include σ_{NI}. These quantities are well known (Ref. 1) for the Rutherford cross section $\sigma_R = \{Z_a Z_b e^2/[\mu_{ab} V^2 \sin^2(\theta/2)]\}^2$ which is the cross section for Coulomb scattering of point particles a and b expressed in terms of the proton numbers Z_a and Z_b, the reduced mass μ_{ab}, and the relative velocity V. The form of the elastic-scattering cross section given, for instance, by Lane and Thomas[14] suggests the exact polynomial expansion for σ_{NI} (Ref. 2),

$$\sigma_{\rm NI}(V,\mu)=-\frac{2\eta}{1-\mu}{\rm Re}\left[\exp\{i\eta\ln[\tfrac{1}{2}(1-\mu)]\}\times\sum_{l=0}^{l_{\rm max}}\frac{2l+1}{2}a_lP_l(\mu)\right]+\sum_{l=0}^{2l_{\rm max}}\frac{2l+1}{2}b_lP_l(\mu)\,, \tag{1}$$

that is truncated at the highest-order partial wave $l_{\rm max}$ that contributes to nuclear scattering. The dependence on the relative velocity enters through the expansion coefficients and through the Coulomb parameter η which is defined as $Z_aZ_be^2/4\pi\epsilon_0\hbar V$, while the dependence on $\mu=\cos\theta$ is explicit in Eq. (1). The Fokker-Planck equation is given by (Ref. 1)

$$\frac{\partial f_a(\vec{v},t)}{\partial t}=-\frac{\partial}{\partial\vec{v}}\cdot\left\langle\frac{\Delta\vec{v}}{\Delta t}\right\rangle f_a+\frac{1}{2}\frac{\partial^2}{\partial\vec{v}\,\partial\vec{v}}:\left\langle\frac{\Delta\vec{v}\,\Delta\vec{v}}{\partial t}\right\rangle f_a \tag{2}$$

and describes the time evolution of a "test" distribution f_a of charged particles of species a which results from their small-angle collisional interaction with "background" charged particles (plasma) of species b. The background distributions f_b enter into the equation through the dynamical friction coefficient $\langle\Delta\vec{v}/\Delta t\rangle$ and through the dispersion tensor $\langle\Delta\vec{v}\,\Delta\vec{v}/\Delta t\rangle$ given, respectively, by

$$\left\langle\frac{\Delta\vec{v}}{\Delta t}\right\rangle=\sum_b\int d\vec{v}_b\int d\vec{\Omega}\,\Delta\vec{v}\,V\sigma_{ab}(V,\vec{\Omega})f_b \tag{3}$$

and

$$\left\langle\frac{\Delta\vec{v}\Delta\vec{v}}{\Delta t}\right\rangle=\sum_b\int d\vec{v}_b\int d\vec{\Omega}\,\Delta\vec{v}\,\Delta\vec{v}\,V\sigma_{ab}(V,\vec{\Omega})f_b\,. \tag{4}$$

In Eqs. (3) and (4), the integrals over the c.m. scattering angle $\vec{\Omega}$ are found to be easily performed analytically if they are first separated into two parts containing the Rutherford terms and the $\sigma_{\rm NI}$ terms, respectively. They subsequently take the forms

$$\left\langle\frac{\Delta\vec{v}}{\Delta t}\right\rangle=-\sum_b\frac{2\pi\mu_{ab}}{m_a}\int d\vec{v}_bf_bV\vec{V}\left[\int_{\mu_0}^{\mu_1}d\mu(1-\mu)\sigma_R+\int_{\mu_0}^{1}d\mu(1-\mu)\sigma_{\rm NI}\right] \tag{5}$$

and

$$\left\langle\frac{\Delta\vec{v}\,\Delta\vec{v}}{\Delta t}\right\rangle=\sum_b\pi\left[\frac{\mu_{ab}}{m_a}\right]^2\int d\vec{v}_bf_bV\left[V_iV_j\left[\int_{\mu_0}^{\mu_1}d\mu\,\sigma_R(3\mu-1)(\mu-1)+\int_{\mu_0}^{1}d\mu\,\sigma_{\rm NI}(3\mu-1)(\mu-1)\right]+\delta_{ij}V^2\left[\int_{\mu_0}^{\mu_1}d\mu\,\sigma_R(1-\mu^2)+\int_{\mu_0}^{1}d\mu\,\sigma_{\rm NI}(1-\mu^2)\right]\right]. \tag{6}$$

The integrals containing the Rutherford cross section have had the standard limits $\mu_1=\cos\theta_{\rm min}$ and $\mu_0=\cos\theta_{\rm max}$ imposed in order to prevent their divergence for very small scattering angles and also in order to constrain the range of integration to small angles. In the $\sigma_{\rm NI}$ integrals, μ_1 may be set to unity since no divergence occurs for $\theta=0$. The relation $\Delta\vec{v}=\mu_{ab}\,\Delta\vec{V}/m_a$ and the fact that σ is azimuthally symmetric in the c.m. system have also been used to write Eqs. (5) and (6).

Substitution of the expressions for σ_R and $\sigma_{\rm NI}$ into Eqs. (5) and (6) results in the generalized expressions for $\langle\Delta\vec{v}/\Delta t\rangle$ and $\langle\Delta\vec{v}\,\Delta\vec{v}/\Delta t\rangle$ given by

$$\left\langle\frac{\Delta\vec{v}}{\Delta t}\right\rangle=\sum_b\Bigg\{\Gamma_{ab}Z_b^2\vec{\nabla}_{\vec{v}}h_{ab}(\vec{v})+\frac{2\pi\mu_{ab}}{m_a}\int d\vec{v}_bf_bV\vec{V}\Bigg[\eta(1-\mu_0){\rm Re}\Bigg[\frac{\exp\{i\eta\ln[\frac{1}{2}(1-\mu_0)]\}}{1+i\eta}\times\sum_{l=0}^{l_{\rm max}}(2l+1)a_l\,{}_3F_2(-l,l+1,1+i\eta;1,2+i\eta,\tfrac{1}{2}(1-\mu_0))\Bigg]$$
$$-\frac{(1-\mu_0^2)^{1/2}}{2}\sum_{l=0}^{2l_{\rm max}}(2l+1)b_l\left[P_l^{-1}(\mu_0)+\frac{1}{(l-1)(l+2)}[(1-\mu_0^2)^{1/2}P_l(\mu_0)+\mu_0P_l^1(\mu_0)]\right]\Bigg]\Bigg\} \tag{7}$$

and

$$\left\langle \frac{\Delta\vec{v}\,\Delta\vec{v}}{\Delta t} \right\rangle = \sum_b \Bigg[\Gamma_{ab} Z_b^2 \vec{\nabla}_{\vec{v}} \vec{\nabla}_{\vec{v}} g_{ab}(\vec{v}) + \pi \left[\frac{\mu_{ab}}{m_a}\right]^2 \int d\vec{v}_b f_b V \Bigg\{ (3V_iV_j - \delta_{ij}V^2) \times \Bigg[\eta \,\mathrm{Re}\left[\sum_{l=0}^{l_{\max}} (2l+1) a_l (1-\mu_0)^2 \exp\{i\eta \ln[\tfrac{1}{2}(1-\mu_0)]\} \frac{\Gamma(2)\Gamma(1+i\eta)}{\Gamma(3+i\eta)} \times {}_3F_2(-l, l+1, 1+i\eta; 1, 3+i\eta, \tfrac{1}{2}(1-\mu_0)) \right] - \sum_{l=0}^{2l_{\max}} \frac{2l+1}{2} b_l (1-\mu_0)^2 \frac{\Gamma^2(2)}{\Gamma(4)} {}_3F_2(-l, l+1, 2; 1, 4, \tfrac{1}{2}(1-\mu_0)) \Bigg]$$

$$+ [(3\mu_0 - 1)V_iV_j - (1+\mu_0)V^2\delta_{ij}] \times \Bigg[\eta \,\mathrm{Re}\left[\sum_{l=0}^{l_{\max}} (2l+1) a_l \frac{1-\mu_0}{1+i\eta} \exp\{i\eta \ln[\tfrac{1}{2}(1-\mu_0)]\} \times {}_3F_2(-l, l+1, 1+i\eta; 1, 2+i\eta, \tfrac{1}{2}(1-\mu_0)) \right]$$

$$- (1-\mu_0{}^2)^{1/2} \sum_{l=0}^{2l_{\max}} \frac{2l+1}{2} b_l \left[P_l^{-1}(\mu_0) + \frac{1}{(l-1)(l+2)} [(1-\mu_0^2)^{1/2} P_l(\mu_0) + \mu_0 P_l^1(\mu_0)] \right] \Bigg] \Bigg\} \Bigg] . \qquad (8)$$

Solutions for the integrals $\int_{\mu_0}^{1}(1-\mu)^{i\eta}P_l(\mu)d\mu$ and $\int_{\mu_0}^{1}(1-\mu)P_l(\mu)d\mu$ in terms of the general hypergeometric functions ${}_3F_2$ and the associated Legendre functions may be found in Ref. 15. In these expressions, Γ_{ab} is given by $Z_a^2 e^4 (\ln\Lambda_b)/4\pi\epsilon_0^2 m_a^2$ where $\ln\Lambda_b$ is the Coulomb logarithm and where the Rosenbluth potentials h_{ab} and g_{ab} are given by

$$h_{ab}(\vec{v}) = \frac{m_a}{\mu_{ab}} \int d\vec{v}_b f_b V^{-1} \qquad (9)$$

and

$$g_{ab}(\vec{v}) = \int d\vec{v}_b f_b V . \qquad (10)$$

Although the Fokker-Planck equation may now be solved for the time evolution of an initial test distribution f_a accounting for nuclear effects, it is more relevant to solve for the time evolution of the average energy of the distribution. This may be accomplished by taking the v^2 moment of Eq. (2) to obtain

$$\langle \dot{v}^2 \rangle \equiv \int d\vec{v}\, v^2 \frac{\partial f_a}{\partial t} = \int d\vec{v} \left[2\vec{v} \cdot \left\langle \frac{\Delta v}{\Delta t} \right\rangle + \overleftrightarrow{\mathbb{1}} : \left\langle \frac{\Delta\vec{v}\,\Delta\vec{v}}{\Delta t} \right\rangle \right] f_a . \qquad (11)$$

Hence, we need only substitute the generalized expressions for $\langle \Delta\vec{v}/\Delta t \rangle$ and $\langle \Delta\vec{v}\,\Delta\vec{v}/\Delta t \rangle$ into Eq. (11) and perform the integral over $d\vec{v}$ in order to calculate $\langle \dot{v}^2 \rangle$ for any initial distribution f_a.

III. RESULTS

For the sake of illustration, the investigation of the effects of nuclear forces in the small-angle scattering regime will be carried out with the example case of fast deuterons slowing down in a tritium plasma. Also, for this purpose, the initial deuteron test-particle distribution will be taken to be monoenergetic and of the form $f_a(\vec{v}) = \delta(\vec{v} - \vec{v}_0)$.

A. The cold ion plasma

For many background plasmas of interest, the ions will be moving at thermal speeds which are much less than the corresponding electron thermal speed even when the plasma is not in equilibrium. Hence, it is often useful to model the background ions as essentially "cold" with respect to the fast incoming ions and also with respect to the "warm" electrons. In this case the background ion distribution may be taken to be of the form $f_i = n_i \delta(\vec{v}_i)$ whereas the background electron distribution may be modeled as a Maxwellian distribution of the form $f_e = n_e(m_e/2\pi kT_e)^{3/2}\exp[-(m_e v_e^2/2kT_e)]$. The quantities $\langle \Delta\vec{v}/\Delta t \rangle$ and $\langle \Delta\vec{v}\,\Delta\vec{v}/\Delta t \rangle$ may be evaluated analytically for distributions of this type and it is straightforward to show that Eq. (11) reduces to

$$\begin{aligned}\langle \dot{v}^2 \rangle = {} & \Gamma_{ae} Z_e^2 n_e \left[\frac{m_a}{\mu_{ae}} \frac{4\alpha_e}{\pi^{1/2}} e^{-\zeta^2} - \frac{m_a}{m_e} \frac{2}{v_0} \Phi(\zeta) \right] - 2\Gamma_{ai} Z_i^2 \frac{n_i m_a}{v_0 m_i} \\ & + \frac{n_i 4\pi v_0^3 \mu_{ai}}{m_a + m_i} \left[\eta(1-\mu_0) \mathrm{Re} \left[\frac{\exp\{i\eta \ln[\frac{1}{2}(1-\mu_0)]\}}{1+i\eta} \right. \right. \\ & \left. \times \sum_{l=0}^{l_{\max}} (2l+1) a_l \, {}_3F_2(-l, l+1, 1+i\eta; 1, 2+i\eta, \tfrac{1}{2}(1-\mu_0)) \right] \\ & \left. - \frac{(1-\mu_0^2)^{1/2}}{2} \sum_{l=0}^{2l_{\max}} (2l+1) b_l \left[P_l^{-1}(\mu_0) + \frac{1}{(l-1)(l+2)} [\, (1-\mu_0^2)^{1/2} P_l(\mu_0) + \mu_0 P_l^1(\mu_0)] \right] \right] . \qquad (12)\end{aligned}$$

Here α_e is the inverse electron thermal speed while ζ is defined as the dimensionless quantity $\alpha_e v_0$.

Equation (12) may be evaluated parametrically in $\vec{v}_0$. If the background electron temperature is set to be 1 keV, the results of this evaluation may be plotted as in Fig. 5. Here the ratio of the time-dependent energy loss resulting from ion-ion nuclear interactions to the time-dependent energy loss resulting from Rutherford ion-ion interactions is plotted as a function of the deuteron's energy in MeV. For this case, the maximum c.m. scattering angle was set to 10° so that $\mu_0 = 0.9848$.

It is seen that this ratio, labeled as $\langle \dot{v}^2 \rangle_{\mathrm{ii\,NI}/R}$, actually decreases to negative values in the lower MeV range of incoming energies. This effect is due to the oscillatory nature of the Coulomb-nuclear interference part of σ_{NI} which dominates in the low MeV and low-scattering-angle regimes (Ref. 2). This is a real effect that has been measured experimentally[16] in some charged particle cross sections and it indeed implies that the traditional ion-ion Fokker-Planck calculations in this energy range are high by some small factor. At about 4.4 MeV, for example, the standard Fokker-Planck ion-ion energy exchange ratio is lowered by about 0.9%.

In Fig. 6, a measurement (Ref. 16) of the elastic-scattering cross section (in this case for p-^{3}He) down to

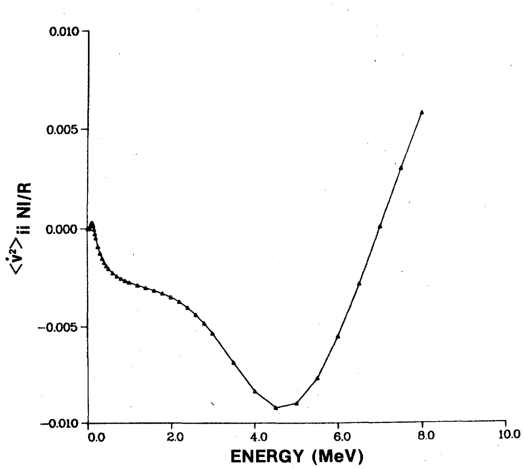

FIG. 5. The ratio of time-dependent energy loss resulting from nuclear and Coulomb-nuclear interference interactions to that resulting from Rutherford interaction for $\mu_0 = \cos(10°)$ in the cold background ion approximation.

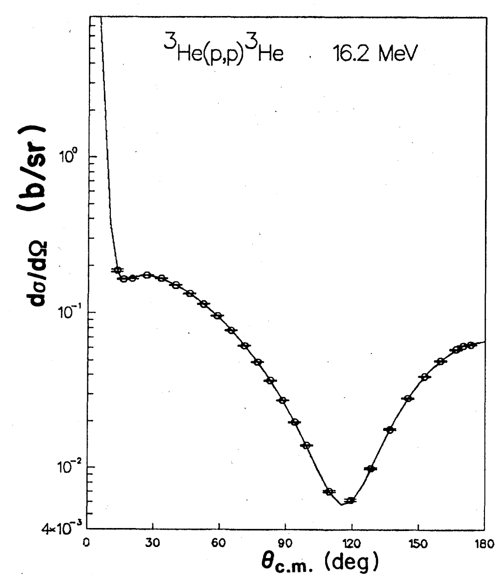

FIG. 6. A measurement of the total differential elastic-scattering cross section for ^{1}H on ^{3}He which clearly indicates an interference minima at $\theta \simeq 15°$ and $E = 16.2$ MeV.

small scattering angles is shown which clearly indicates this interference minimum. The solid curve in this figure was also fit by means of Eq. (1).

Returning to Fig. 5, it is seen that in the upper MeV range the ratio $\langle \dot v^2\rangle_{\rm ii\,NI/R}$ climbs to values about 0.5% higher than the Rutherford estimate at 8 MeV. Hence, at this energy, the correction to standard Fokker-Planck ion-ion energy exchange calculations would be positive. It should be noted, though, that at these higher energies where the corrections amount to an actual increase in the ion-ion energy exchange rate, the rate of ion-electron energy exchange would also be large. At 8 MeV, for example, $v_0 > v_e > v_i$ and it is a well-known result that the ion-electron Rutherford energy exchange rate remains large until $v_e > v_0 > v_i$.[17]

In Fig. 7 the same ratio is plotted for a case in which the maximum c.m. scattering angle is now chosen to be 30° ($\mu_0 = 0.866$). The dramatic difference in these results, as compared to those in Fig. 5, indicate that the energy exchange rate is very sensitive to the choice of cutoff angle. For this case, it is seen that the pure Rutherford calculation of $\langle \dot v^2\rangle$ underpredicts the amount of ion-ion heating by a factor of 2 at energies around 7 MeV. At 8 MeV the correction to the heating rate becomes closer to 150%.

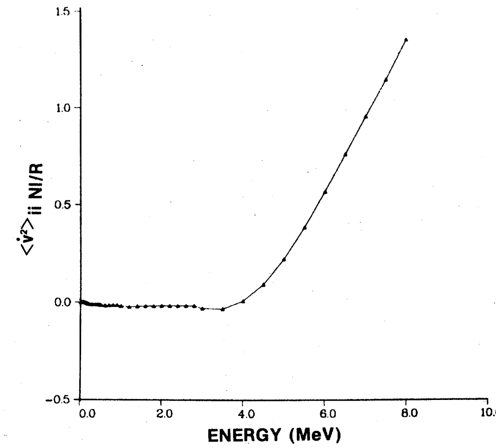

FIG. 7. The ratio of time-dependent energy loss resulting from nuclear and Coulomb-nuclear interference interactions to that resulting from Rutherford interaction for $\mu_0 = \cos(30°)$ in the cold background ion approximation.

B. The hot ion plasma

For cases in which the speeds of the background plasma particles are comparable (i.e., nonequilibrium backgrounds) or for which the initial test ions' speeds are comparable to the background ions' speeds, the plasma must be modeled with realistic ion and electron distributions.

The evaluation of Eq. (11) remains tractable when these distributions may both be chosen to be Maxwellian. In the following, the general case in which the background electrons and ions have separate Maxwellian temperatures T_e and T_i will be addressed. For this case, it is also straightforward to show that Eq. (11) reduces to

$$
\begin{aligned}
\langle \dot v^2\rangle = \sum_b \Bigg\{ & \Gamma_{ab} Z_b^2 n_b \left[\frac{m_a}{\mu_{ab}} \frac{4\alpha_b}{\pi^{1/2}} e^{-\zeta_b^2} - 2\frac{m_a}{m_b}\frac{\Phi(\zeta_b)}{v_0} \right] \\
& + 8\pi^2 n_b \left[\frac{\alpha_b^2}{\pi}\right]^{3/2} \int_0^\infty dV\, V^2 \left[e^{\gamma_1} \frac{\mu_{ab}}{m_a a_b} \left[v - \frac{v}{a_b} - \frac{\mu_{ab}}{m_a} V \right] + e^{\gamma_2} \frac{\mu_{ab}}{m_a a_b} V^2 \left[v + \frac{v}{a_b} + \frac{\mu_{ab}}{m_a} V \right] \right] \\
& \times \Bigg[\eta(1-\mu_0) \mathrm{Re} \left[\frac{\exp\{ i\eta \ln[\tfrac{1}{2}(1-\mu_0)]\}}{1+i\eta} \right. \\
& \qquad \left. \times \sum_{l=0}^{l_{\max}} (2l+1) a_l\, {}_3F_2(-l, l+1, 1+i\eta; 1, 2+i\eta, \tfrac{1}{2}(1-\mu_0)) \right] \\
& \qquad - \frac{(1-\mu_0^2)^{1/2}}{2} \sum_{l=0}^{2l_{\max}} (2l+1) b_l \left[P_l^{-1}(\mu_0) + \frac{1}{(l-1)(l+2)} [(1-\mu_0^2)^{1/2} P_l(\mu_0) + \mu_0 P_l^1(\mu_0)] \right] \Bigg] \Bigg\} . \qquad (13)
\end{aligned}
$$

In this result, the sum over background species b should be taken for both background electrons and ions in the first term (the Rutherford term) but, of course, only over background ion species in the remaining terms which contain the ion-ion nuclear effects. The following definitions have also been introduced: $a_b = 2\alpha_b^2 v_0 V$, $\gamma_1 = \alpha_b^2 (v_0 - V)^2$, and $\gamma_2 = -\alpha_b^2 (v_0 + V)^2$. It can be shown that in the limit of zero background ion temperature Eq. (13) reduces to Eq. (12).

In Eq. (13) the integral over the relative speed may be performed numerically. Figures 8 and 9 contain the results in terms of the ratio $\langle \dot v^2\rangle_{\rm ii\,NI/R}$ for a case in which both of the background temperatures were set equal to 1 keV but for which μ_0 was set to the cosines of 10° and 30°,

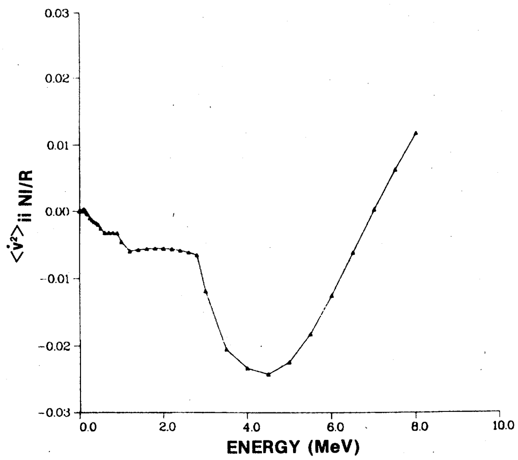

FIG. 8. The ratio of time-dependent energy loss resulting from nuclear and Coulomb-nuclear interference interactions to that resulting from Rutherford interaction for $\mu_0=\cos(10°)$ where $T_e=T_i=1$ keV.

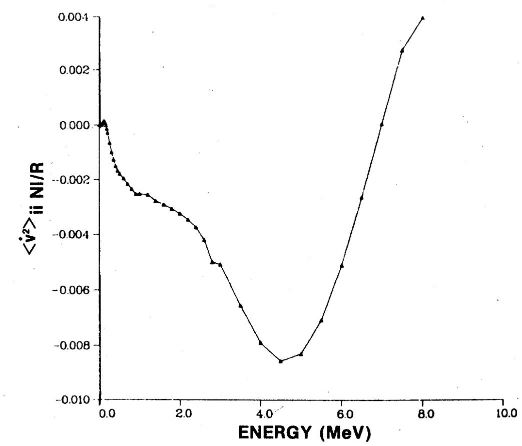

FIG. 10. The ratio of time-dependent energy loss resulting from nuclear and Coulomb-nuclear interference interactions to that resulting from Rutherford interaction for $\mu_0=\cos(10°)$ where $T_e=T_i=10$ keV.

respectively. The small corrections, both positive and negative, are again seen for the case in which $\mu_0=0.9848$ (Fig. 8) but corrections as high as 70% are seen at 8 MeV for $\mu_0=0.866$ in Fig. 9.

If the background temperatures are both increased to 10 keV, the corrections for the cases in which $\mu_0=\cos(10°)$ and $\cos(30°)$, respectively, are shown in Figs. 10 and 11. In the case where $\mu_0=0.866$ (Fig. 11), it is seen that the correction at 8 MeV amounts to about 50%.

IV. CONCLUSIONS

It has been shown that Fokker-Planck theory may be generalized to include the effects of nuclear forces in the small-angle scattering regime. This has been accomplished through the addition of the Coulomb-nuclear interference and the nuclear elastic-scattering cross sections to the Rutherford cross section in the scattering integrals of the Fokker-Planck equation.

Corrections to the ion-ion energy exchange rate which previously included only the effects of Rutherford scattering were found to be quite sensitive to the choice of a cutoff angle θ_{max} in the range of scattering angles $\theta_{min} \leq \theta \leq \theta_{max}$ over which the theory may be applicable. Within the angular range over which the effects of nuclear forces have been investigated ($10° \leq \theta_{max} \leq 30°$), it was found that corrections as large as 150% are predicted for the energy exchange rate between D and T ions. It is expected that similar results would be obtained for other light charged particle pairs, based on the behavior of σ/σ_R over the same angular range. These large correc-

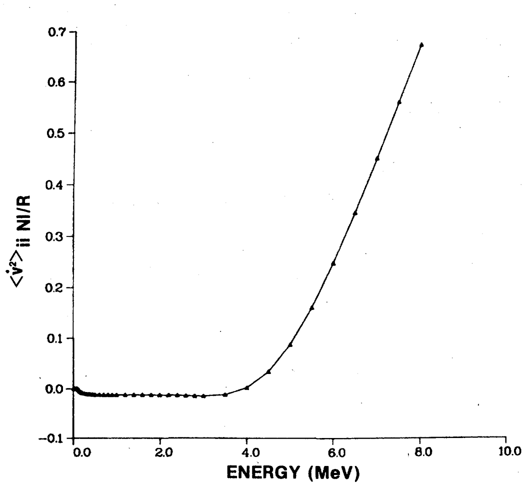

FIG. 9. The ratio of time-dependent energy loss resulting from nuclear and Coulomb-nuclear interference interactions to that resulting from Rutherford interaction for $\mu_0=\cos(30°)$ where $T_e=T_i=1$ keV.

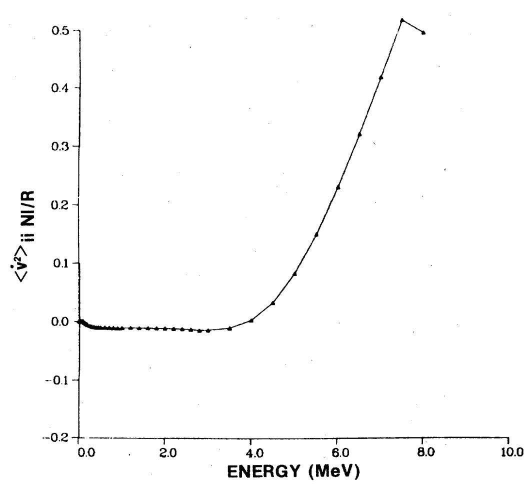

FIG. 11. The ratio of time-dependent energy loss resulting from nuclear and Coulomb-nuclear interference interactions to that resulting from Rutherford interaction for $\mu_0=\cos(30°)$ where $T_e=T_i=10$ keV.

tions to the ion-ion energy loss generally occur in the velocity regime where ion-electron losses dominate; however, significant increases in the predicted ion heating may be important for some plasma devices even in this regime.

Although this generalized theory now provides for a smooth connection between small- and large-angle ion slowing calculations, a more precise determination of the cutoff angle θ_{max} remains to be done. This determination would be of importance to researchers in fusion reactor design, for example, in which Fokker-Planck theory is typically used to model the time evolution of a plasma that results from ion heating to thermonuclear conditions.

A further generalization of this theory may, in principle, be possible. An approach similar to the one employed here might be used to formulate a Fokker-Planck equation which would describe the collisional evolution of a distribution of spin polarized particles in the small-angle scattering regime. Although a new expansion for σ_{NI}, in which the coefficients would not be averaged over spin, would be necessary, the principles of generalizing $\langle \Delta\vec{v}/\Delta t \rangle$ and $\langle \Delta\vec{v}\,\Delta\vec{v}/\Delta t \rangle$ over a small range of angles would remain the same.

---

[1]M. N. Rosenbluth, W. M. MacDonald, and D. L. Judd, Phys. Rev. **107**, 1 (1957).

[2]G. M. Hale, D. C. Dodder, and J. C. DeVeaux, in *Proceedings of the International Conference on Nuclear Data for Science and Technology, Antwerp, Belgium, 1982,* edited by K. H. Böckhoff (Reidel, Dordrecht, Holland, 1983), p. 326.

[3]J. M. Blair, G. Freier, E. Lampi, W. Sleator, and J. H. Williams, Phys. Rev. **74**, 1594 (1948).

[4]A. S. Wilson, M. C. Taylor, J. C. Legg, and G. C. Phillips, Nucl. Phys. **A126**, 193 (1969).

[5]M. Ivanovich, P. G. Young, and G. G. Ohlsen, Nucl. Phys. **A110**, 441 (1968).

[6]W. R. Stratton, D. G. Freier, G. R. Keepin, D. Rankin, and T. F. Stratton, Phys. Rev. **88**, 257 (1952).

[7]A. Galonsky, R. A. Douglas, W. Haeberli, M. T. McEllistrem, and H. T. Richards, Phys. Rev. **98**, 586 (1955).

[8]L. S. Senhouse and T. A. Trombello, Nucl. Phys. **57**, 624 (1964).

[9]G. G. Ohlsen and P. G. Young, Nucl. Phys. **52**, 134 (1964).

[10]N. A. Krall and A. W. Trivelpiece, *Principles of Plasma Physics* (McGraw-Hill, New York, 1973), p. 293.

[11]F. Evans, Phys. Fluids **16**, 1011 (1973).

[12]A. Andrade, Ph.D. dissertation, University of Michigan, 1981.

[13]S. T. Perkins and D. E. Cullen, Nucl. Sci. Eng. **77**, 20 (1981).

[14]A. M. Lane and R. G. Thomas, Rev. Mod. Phys. **30**, 257 (1958).

[15]I. S. Gradshteyn and I. M. Ryzhik, *Tables of Integrals, Series, and Products* (Academic, New York, 1965), pp. 794, 795, and 823.

[16]R. L. Hutson, N. Jarmie, J. L. Detch, Jr., and J. H. Jett, Phys. Rev. C **4**, 17 (1971).

[17]S. T. Butler and M. J. Buckingham, Phys. Rev. **126**, 1 (1962).